Plant Physiology, 2026, 201, 1–10
https://doi.org/10.1093/plphys/kiag600
Published: 17 August 2026
Research Report

Plant Physiology®

The yellow-in-the-dark *chlL* Chlamydomonas mutant as a model for time-resolved chloroplast biogenesis and retrograde signaling

M. Águila Ruiz-Sola [1,2,3*‡], Mariano A. De Silvio [1], Mario Becerra-Tinoco [2], Andrea M. Quintero-Moreno [2], Beatrice Pacenza [1], José L. Crespo [2], and Elena Monte [1,4*‡§]

[1]Centre for Research in Agricultural Genomics (CRAG) CSIC-IRTA-UAB-UB, Campus UAB, Bellaterra, Barcelona 08193, Spain
[2]Instituto de Bioquímica Vegetal y Fotosíntesis, Universidad de Sevilla-CSIC, Av. Américo Vespucio 49, Sevilla 41092, Spain
[3]Departamento de Bioquímica Vegetal y Biología Molecular, Facultad de Química, Universidad de Sevilla, Calle Profesor García González 1, Sevilla 41012, Spain
[4]Consejo Superior de Investigaciones Científicas (CSIC), Barcelona 08028, Spain

*Corresponding authors: M. Águila Ruiz-Sola, Instituto de Bioquímica Vegetal y Fotosíntesis, Universidad de Sevilla-CSIC, Av. Américo Vespucio 49, Sevilla 41092, Spain. Email: mrsola@us.es; Elena Monte, Centre for Research in Agricultural Genomics (CRAG) CSIC-IRTA-UAB-UB, Campus UAB, Bellaterra, Barcelona 08193, Spain; Consejo Superior de Investigaciones Científicas (CSIC), Barcelona 08028, Spain. Email: elena.monte@cragenomica.es
‡Authors for communication.
§Senior author
The authors responsible for distribution of materials integral to the findings presented in this article in accordance with the policy described in the Instructions for Authors (https://academic.oup.com/plphys/pages/General-Instructions) are M. Águila Ruiz-Sola (M.Á.R-S.) and Elena Monte (E.M.).

Abstract

Understanding chloroplast biogenesis is key given the importance of photosynthesis and chloroplast metabolism. Chloroplast assembly has been extensively studied in angiosperms, where the main hallmarks have been established, including the need for nuclear and plastid genome coordination through anterograde and retrograde signals. However, recent works in other photosynthetic lineages have revealed both divergent and conserved regulators. These differences likely represent adaptive strategies that emerged during the evolution of the green lineage and highlight the need for evolutionary studies to fully elucidate the mechanisms controlling chloroplast biogenesis, a light-promoted process. Here, we characterize the yellow-in-the-dark *chlL* mutant of *Chlamydomonas reinhardtii*, which carries a mutation in the CHLL subunit of the dark-operative POR enzyme. Dark-adapted *chlL* cells cannot synthesize chlorophylls and display a de-differentiated chloroplast, and our results show that upon exposure to light, chloroplast biogenesis is initiated very rapidly based on starch reserves. We demonstrate that accumulation of pigments, photosynthesis-related proteins, and functional chloroplast activity is detected within 1 to 3 h of illumination. Additionally, we show that lincomycin, an inhibitor of plastid translation, specifically affects chloroplast physiology, blocks light-induced chloroplast biogenesis and cell growth, and triggers retrograde signaling, establishing lincomycin as a valuable tool for investigating chloroplast physiology and plastid-to-nucleus communication in Chlamydomonas. Together, this study introduces the *chlL* mutant as a powerful model system to dissect light-induced, time-resolved chloroplast biogenesis, as well as the responses and signaling triggered by lincomycin. By promoting broader adoption of this model, we aim to help inform strategies to enhance photosynthesis and stress tolerance and optimize bioproduct production.

Introduction

Chloroplasts house photosynthesis and function as metabolic hubs necessary for pigment biosynthesis and production of vital metabolites (Rolland et al. 2018). Understanding chloroplast biogenesis is key to establish the basis of photosynthetic and metabolic competence, essential for adaptation to changing environments and global primary production.

Chloroplast biogenesis has been extensively studied in angiosperms. Dark-grown etiolated seedlings accumulate etioplasts featuring a prolamellar body, which harbors the chlorophyll precursor protochlorophyllide (Pchlide) and the nuclear-encoded, light-dependent enzyme Pchlide oxidoreductase (LPOR) that controls the reduction of Pchlide to chlorophyllide (Chlide) in the light (Floris and Kühlbrandt 2021). Consequently, etiolated seedlings lack chlorophylls and exhibit a yellowish color, a characteristic of carotenoids. Upon exposure to light, etioplasts develop into green chloroplasts, and seedlings undergo de-etiolation to promote optimal photosynthetic performance (Gommers and Monte 2018).

Received: December 17, 2025. **Accepted:** August 7, 2026
© The Author(s) 2026. Published by Oxford University Press on behalf of American Society of Plant Biologists.
This is an Open Access article distributed under the terms of the Creative Commons Attribution-NonCommercial-NoDerivs licence (https://creativecommons.org/licenses/by-nc-nd/4.0/), which permits non-commercial reproduction and distribution of the work, in any medium, provided the original work is not altered or transformed in any way, and that the work is properly cited. For commercial re-use, please contact reprints@oup.com for reprints and translation rights for reprints. All other permissions can be obtained through our RightsLink service via the Permissions link on the article page on our site—for further information please contact journals.permissions@oup.com.

Downloaded from academic.oup.com/plphys/article/201/4/kiag600/8762110 by guest on 28 August 2026

In contrast to flowering plants, most of the remaining major groups of the green lineage retain the capacity to produce chlorophyll in the dark, thanks to a light-independent dark-operative pchlide oxidoreductase (DPOR) (Vedalankar and Tripathy 2019). DPOR is plastid encoded and consists of 3 subunits (CHLN, CHLB, and CHLL), which catalyze the light-independent reduction of Pchlide to Chlide (Armstrong 1998). DPOR activity has been lost entirely in angiosperms and partially in gymnosperms and some algae (Solymosi and Schoefs 2010; Hunsperger et al. 2015). Importantly, chlorophyte algae, including the model organism *Chlamydomonas reinhardtii*, retain high DPOR prevalence and are green with morphological features of the chloroplast similar to light-grown cells even after prolonged darkness (Sager and Palade 1954).

Numerous studies in angiosperms have defined the hallmarks of chloroplast biogenesis (Jarvis and López-Juez 2013; Pipitone et al. 2021), which include the coordinated synthesis and import of the chloroplast protein machinery encoded in the nuclear genome, along with the massive production of lipids and chlorophylls in the chloroplast to drive the assembly of photosynthetic complexes and thylakoid membranes. Light is essential for activating the transcriptomic reprogramming necessary for chloroplast biogenesis, and many of the regulators have been elucidated, including the master regulators GLKs (Frangedakis et al. 2024; Waters et al. 2009). Recent works in other photosynthetic lineages have revealed both divergent and conserved regulators, including some previously overlooked in Arabidopsis (Nishiyama et al. 2018; Frangedakis et al. 2024). Such differences likely reflect adaptive strategies that emerged throughout the evolution of the green lineage, highlighting the need for comparative studies to fully uncover the mechanisms that control light-regulated chloroplast biogenesis.

The unicellular green alga *C. reinhardtii*, featuring a single chloroplast with thylakoid architecture and composition similar to higher plants, provides a powerful system to explore the evolutionary foundations of chloroplast biogenesis (Ostermeier et al. 2024). Chlamydomonas can grow nonphotosynthetically in the dark in acetate-containing media while maintaining a green and functional chloroplast due to DPOR activity (Harris 2001). Importantly, the yellow-in-the-dark mutant *y-1*, with defects in the accumulation of the DPOR subunit CHLL, was used to pioneer investigations into light-regulated chloroplast biogenesis (Sager and Palade 1954; Ohad et al. 1967a; Cahoon and Timko 2000). Similar to etiolated seedlings, *y-1* is yellowish with undifferentiated plastids that accumulate Pchlide and carotenoids in darkness and fully develop into functional chloroplasts upon illumination (Ohad et al. 1967b; Malnoë et al. 1988; White and Hoober 1994). Unfortunately, the genetic basis of *y-1* remains unknown, hindering its use as a model. This was addressed by targeted chloroplast mutations in the DPOR CHLL subunit, which generated the yellow-in-the-dark *chlL* mutant (Suzuki and Bauer 1992). However, chloroplast biogenesis in this *chlL* mutant remains to be characterized.

The antibiotic lincomycin inhibits protein synthesis in the chloroplast and has been extensively used in plants to study chloroplast development and the coordination of nuclear and plastid genomes (León et al. 2025). In contrast, the use of lincomycin to study chloroplast biogenesis and signaling in Chlamydomonas has not been explored.

Here, we describe a detailed methodology to establish the *chlL* mutant as a model system to study time-resolved light-induced chloroplast biogenesis. We provide a comprehensive physiological and biochemical analysis of chloroplast biogenesis in *chlL* from a dark undifferentiated plastid to a fully functional chloroplast. Furthermore, we show that the antibiotic lincomycin is a valuable tool for investigating the process of chloroplast biogenesis in Chlamydomonas.

Results

Lincomycin impacts Chlamydomonas growth and physiology

Wild-type strains CC-124 and CC-3269 were grown on the acetate-containing TAP and Tris-phosphate (TP) minimum medium plates in continuous light (TAP Light and TP Light) or darkness (TAP Dark) in the presence or absence of lincomycin. Growth in TP Light was slower compared to TAP Light as expected, whereas growth in TAP Dark took longer, as shown in the serial spot dilutions in Fig. 1a depicting cells grown for different lengths of time to reach similar growth: 6 (TP), 5 (TAP), and 12 (TAP Dark) days. In light conditions, the presence of lincomycin considerably affected growth, whereas in darkness, lincomycin did not appear to have a visible impact (Fig. 1a). CC-124 grown under the same conditions in liquid medium (Fig. 1b) showed exponential growth after inoculation (Day 0) in TAP Light from Day 1 to Day 3, when it reached a plateau. In TP Light, and even more in TAP Dark, growth was slower (Fig. 1b), mirroring the dynamics on plates (Fig. 1a). Likewise, addition of lincomycin prevented growth only in light conditions (Fig. 1b). Corresponding growth rates showed an increase between Days 0 and 2 in TAP Light and Dark, and between Days 0 and 3 in TP Light, with a subsequent drop (Fig. 1c). Again, lincomycin-treated samples showed reduced growth rate only in light samples (Fig. 1c). Together, our results show that lincomycin impairs the growth of WT Chlamydomonas strains in the light in both acetate-containing and minimal media, whereas no significant effect was detected under dark conditions. This lack of lincomycin effect in the dark might reflect the reduced need for chloroplast translation during heterotrophic growth, with most essential chloroplast biosynthetic functions (apart from photosynthesis) relying on nuclear-encoded proteins. We next complemented the growth data with physiological measurements at Day 1. Chlorophyll content was similar in TAP Light and TP Light, but reduced in TAP Dark, and lincomycin treatment triggered a decrease in all 3 growth conditions (Fig. 1d). Measurement of photosynthetic oxygen evolution rates indicated that TAP Light and TP Light cells exhibited similar photosynthetic capacity (Fig. 1d), while TAP Dark cells had reduced levels. Interestingly, in all 3 conditions, photosynthesis was affected by lincomycin (Fig. 1d). Finally, mitochondrial respiration, measured by assessing oxygen consumption rates in the dark, showed some differences among light treatments, likely reflecting distinct mitochondrial activity during mixotrophic, autotrophic, and heterotrophic growth, but remarkably, no differences were observed between lincomycin-treated and nontreated samples in each condition. Our results indicate that lincomycin can impact chlorophyll content and photosynthesis in cells grown in both light and dark, and this effect on chloroplast physiology appears to be specific, as lincomycin does not significantly affect respiration.

Chloroplast structure and pigment profile of the yellow-in-the-dark *chlL* mutant under different light regimes

chlL growth in TAP Light, TP Light, and TAP Dark showed similar growth patterns compared to the wild-type (WT) control CC-3269 (Fig. 2a), indicating that *chlL* cells can grow and divide in both light and dark conditions. We next established a detailed protocol to

Downloaded from academic.oup.com/plphys/article/201/4/kiag600/8762110 by guest on 28 August 2026

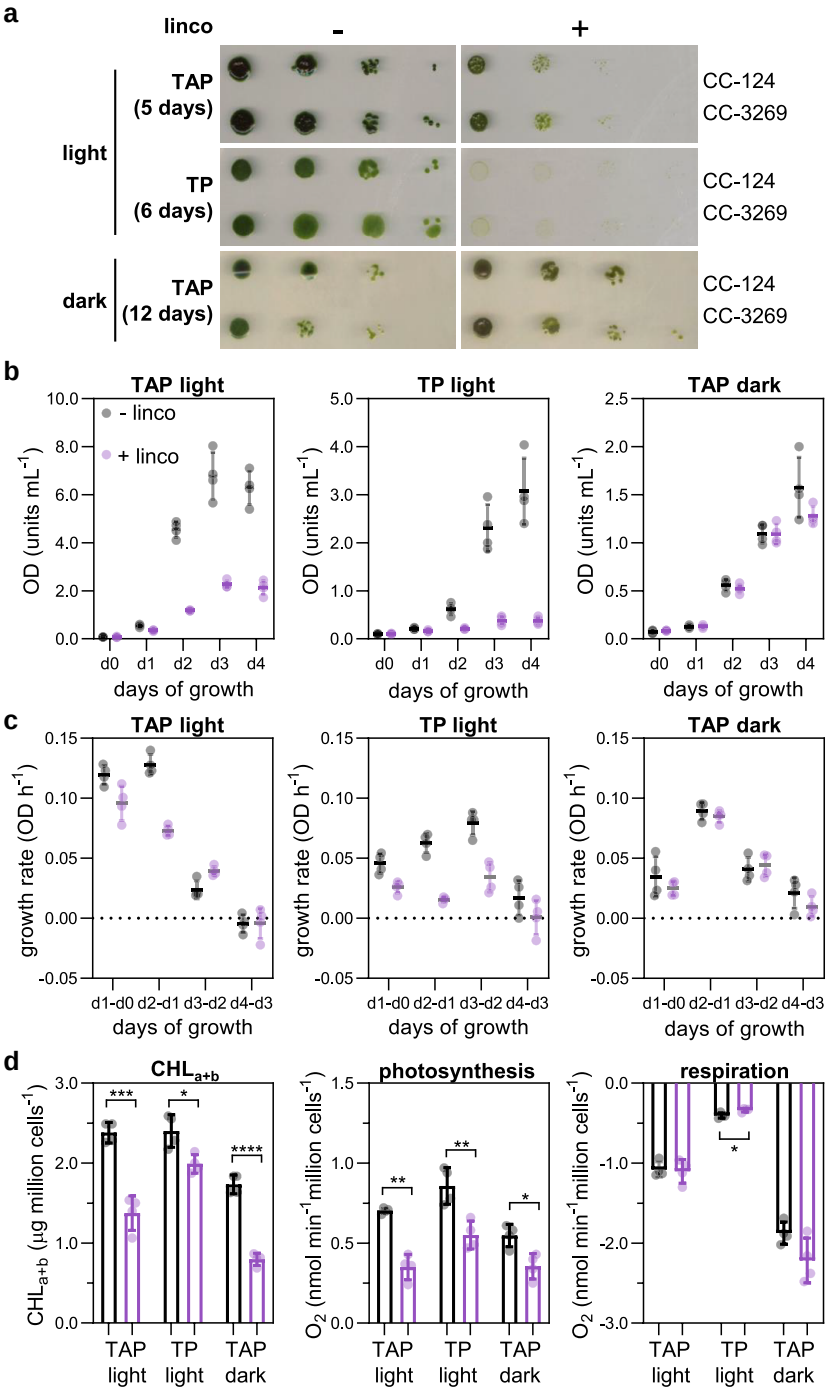

Figure 1 Lincomycin affects Chlamydomonas growth and physiology. a) Growth of Chlamydomonas strains CC-124 and CC-3269 under continuous light in solid TAP (5 d) and TP (6 d) media, or under continuous darkness on TAP (12 d). Cells were subjected to 10-fold serial dilutions and spotted into plates with or without lincomycin 0.5 mM (Linco). b) Growth curves of CC-124 grown in liquid medium as in (a), for 0, 1, 2, 3, and 4 d after inoculation, expressed as $O.D._{750}$ units/mL. c) Growth rate (expressed as $O.D._{750}$ units/hour) of cultures grown in (b). d) Total chlorophyll content expressed in microgram per million cells, and the rate of oxygen evolution and consumption expressed in nanomole O_2 per minute per million cells of CC-124 cells after 1 d of growth as in (b). Asterisks denote statistically significant differences (*t*-test.*$P \leq 0.05$; **$P \leq 0.01$; ***$P \leq 0.001$; ****$P \leq 0.0001$).

characterize the physiology and subcellular features of the *chlL* mutant grown under our conditions of prolonged darkness and transfer to light (Fig. 2b). *chlL* grown on TAP Light plates was used to inoculate a liquid TAP culture and placed in continuous darkness. Under these conditions, the *chlL* mutant turned yellowish after 5 d (Fig. 2c), as expected due to its DPOR deficiency, which prevents chlorophyll accumulation in the dark (Suzuki and Bauer 1992). However, in agreement with LPOR activation upon light illumination, dark-grown *chlL* cultures transferred to TP and light for 48 h were green and indistinguishable from continuous light-grown *chlL* (Fig. 2c).

At the subcellular level, dark-grown *chlL* cells exhibited a partially developed chloroplast that lacked thylakoid membranes and grana

Downloaded from academic.oup.com/plphys/article/201/4/kiag600/8762110 by guest on 28 August 2026

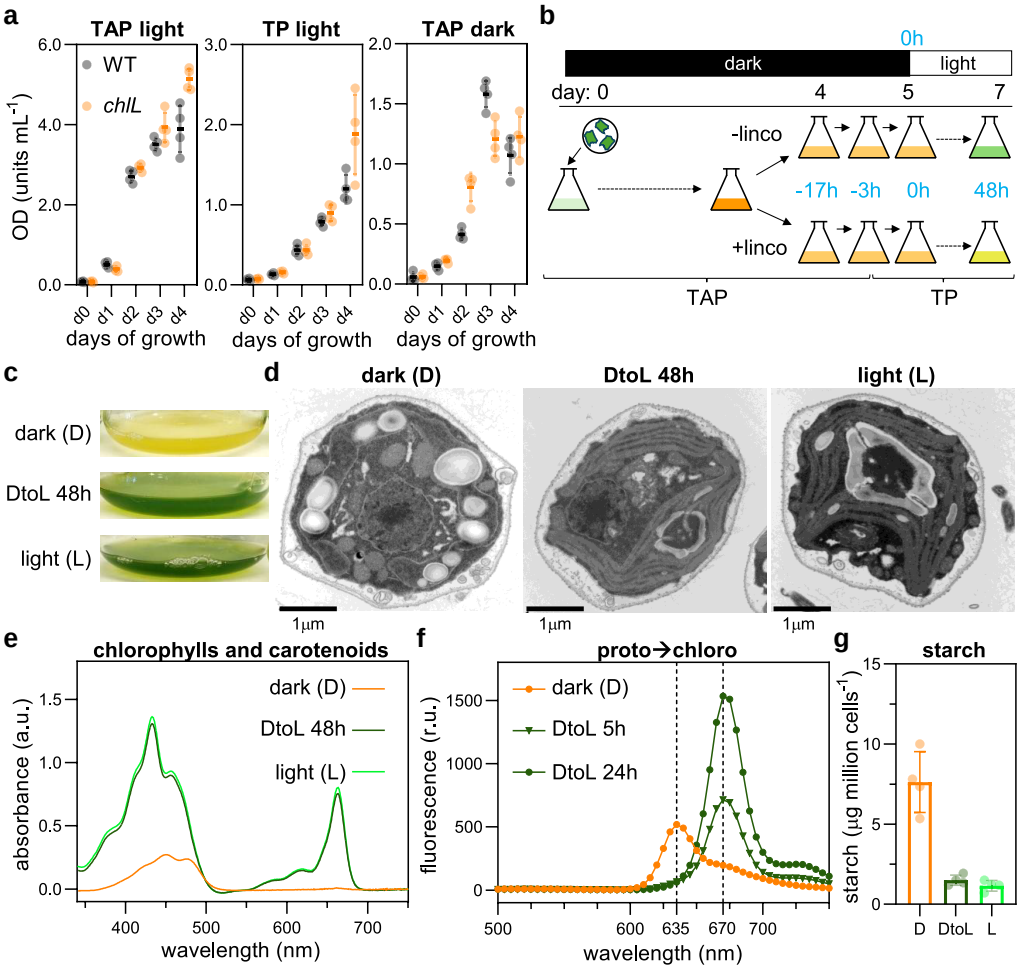

Figure 2 Chloroplast structure and pigment profile of the *chlL* mutant. a) Growth of Chlamydomonas strains CC-3269 and *chlL* in liquid TAP or TP media in continuous light, or under continuous darkness in TAP for 0, 1, 2, 3, and 4 d after inoculation, expressed as $O.D._{750}$ units/mL. b) Schematic representation of the established protocol to grow the *chlL* mutant in the dark to induce the loss of chlorophylls and chloroplast dedifferentiation. c) Appearance of liquid cultures of *chlL* cells grown for 7 d in TAP medium in the dark (top), for 7 d under continuous light in TP (bottom), or grown in the dark for 5 d in TAP and then transferred to light in TP for 48 h (middle). d) TEM images of *chlL* cells grown as in (b). e) Absorbance spectra of *chlL* cells grown as in (b), with values expressed as arbitrary units (a.u.). f) Fluorescence spectrum after excitation at 440 nm of dark-grown *chlL* cells (0 h) transferred to light for 5 and 24 h, expressed as relative units (r.u.). (g) Starch content of *chlL* cells grown as in (b), expressed as microgram of starch per million cells.

stacks (Fig. 2d), similar to the *y-1* mutant (Ohad et al. 1967a). Dark-grown *chlL* cells transferred to light for 48 h showed fully developed cup-shaped chloroplasts with thylakoid membranes stacked in grana, like *chlL* cells grown under continuous light (Fig. 2d) and comparable to well-documented WT cells (Broderson et al. 2024). Photosynthetic pigment accumulation in all 3 conditions was in accordance with these phenotypes: Dark-grown *chlL* mutant showed accumulation of carotenoids but no chlorophylls (Fig. 2e), whereas dark-grown *chlL* cells transferred to light for 48 h and light-grown *chlL* cells accumulated carotenoids and chlorophylls to similar amounts (Fig. 2e). During the dark-to-light conditions, the chlorophyll precursor Pchlide is rapidly transformed into Chlide by the LPOR enzyme (Fig. 2f). Together, these results indicate that dark-grown yellow *chlL* cells transferred to light accumulate chlorophyll and develop a structured chloroplast similar to *chlL* cells grown light under continuous. Interestingly, we observed the presence of starch granules in TAP Dark that were absent after 48 h of light, presumably consumed to fuel chloroplast biogenesis (Fig. 2d and g), similar to what has been described in dark-grown cell cultures of angiosperms (Dubreuil et al. 2018; Gillott et al. 1991).

Dark-grown yellow *chlL* mutant rapidly builds a functional chloroplast when exposed to light, a process impaired in the presence of lincomycin

To establish the timing and physiology of chloroplast biogenesis in *chlL*, cells were first grown in continuous darkness until yellow and were then transferred to continuous light (time point = 0 h) for 48 h, sampling after 1, 3, 6, 9, 24, and 48 h (Fig. 2b). A separate culture of *chlL* cells was grown under continuous light as a reference control. Throughout the dark-to-light time-course, cells looked healthy, and greening was progressive and visually apparent after 3 to 6 h (Fig. 3a and b), with no signs of stress from light exposure either morphologically (Fig. 3a) or molecularly (Fig. S1), and with cell division, measured as total cell count, detectable 9 to 12 h after lights on (Fig. 3c). Chlorophyll and carotenoid accumulation (Fig. 3d and e),

Downloaded from academic.oup.com/plphys/article/201/4/kiag600/8762110 by guest on 28 August 2026

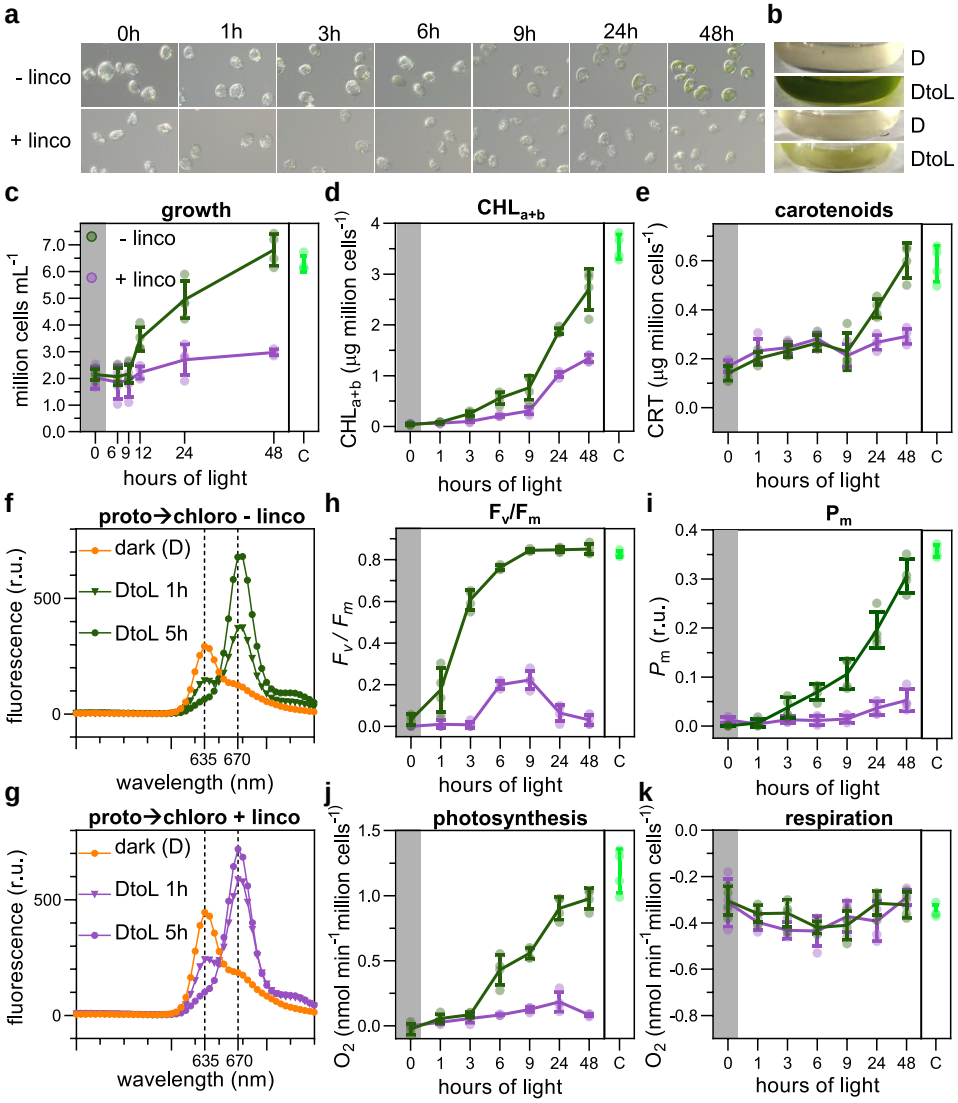

Figure 3 Time-resolved physiology of chloroplast biogenesis in the dark-adapted *chlL* mutant upon transfer to the light in the presence or absence of lincomycin (linco). a) Light micrographs of dark-grown *chlL* cells in liquid cultures exposed to continuous light for the indicated times [0 {Dark}, 1, 3, 6, 9, 24, and 48 h], in the presence (bottom) or absence (top) of lincomycin. b) Appearance of *chlL* cultures grown as in (a). DtoL (Dark to Light) correspond to samples after 48 h. c) Growth curves expressed as cell number (million cells per milliliter). d) Total chlorophyll content expressed in microgram per million cells. e) Total carotenoid content expressed in microgram per million cells. f and g) Fluorescence spectrum after excitation at 440 nm of dark-grown *chlL* cells (0 h) transferred to light for 1 and 5 h, expressed as relative units (r.u.) in the absence f) and presence g) of lincomycin. h) F_v/F_m values. i) P_m values expressed in relative units (r.u.). j) Rate of oxygen evolution expressed in nanomole O_2 per minute per million cells. k) Rate of oxygen consumption expressed in nanomole O_2 per minute per million cells. Green lines correspond to light-treated samples. Purple lines correspond to lincomycin-treated samples. The light green sample corresponds to the control (c) *chlL* mutant grown under continuous light.

Pchlide to Chlide conversion (Fig. 3f and g), and the assembly of functional photosystem (PS) PSII and PSI [as shown by the maximum photochemical efficiency of PSII {F_v/F_m} and the maximum amount of photo-oxidizable P700 {P_m} values, respectively] were detected as early as 1 to 3 h after light onset (Fig. 3h and i; Fig. S2). Accordingly, photosynthetic activity, measured by the oxygen evolution rate, was detected after 3 to 6 h (Fig. 3j). Complete chloroplast biogenesis was reached after 48 h, when physiological values were similar to control *chlL* cells grown under continuous light (Fig. 3d to e and 3h to j). Overall, physiological values of our *chlL* system were comparable to, and expanded upon, previous studies using other *yellow-in-the-dark* genotypes (Ohad et al. 1967b; White and Hoober 1994). For comparison, we analyzed dark-grown WT cells transferred to light. As expected, given the retention of a structured chloroplast in the dark in WT cells (Sager and Palade 1954), WT physiological values did not change significantly upon illumination (Fig. S3). Addition of lincomycin to the system (Fig. 2b) had a clear impact on greening (Fig. 3a and b). Although rapid Pchlide-to-Chlide conversion was not affected (Fig. 3f and g), lincomycin impaired the accumulation of chlorophylls and carotenoids, PS assembly and activity, and cell division (Fig. 3c to e and 3h to j; Fig. S2). Interestingly, lincomycin increased F_0 values, suggesting the presence of free chlorophylls due to impaired PS assembly (Fig. S2). However, increased F_0 may also indicate that a fraction of chlorophyll is not efficiently coupled to PSII, consistent with incomplete assembly of PSII complexes and thylakoid membranes during chloroplast biogenesis in the presence of lincomycin. Importantly, O_2 consumption rate due to respiration showed similar values in all samples (Fig. 3k), indicating that the effect of lincomycin is highly

Downloaded from academic.oup.com/plphys/article/201/4/kiag600/8762110 by guest on 28 August 2026

specific to the chloroplast. In short, dark-grown yellow *chIL* cells rapidly assemble a functional chloroplast upon light exposure, a process impaired by the addition of lincomycin.

Light induces early accumulation of photosynthesis-related proteins during chloroplast biogenesis

To further understand the dynamics of light-induced chloroplast assembly, we next assessed the accumulation of key photosynthesis-related proteins in dark-grown yellow *chIL* cells exposed to light after 0, 3, 6, 9, 24, and 48 h of light treatment and compared them to *chIL* grown under continuous light as a control. Evaluated proteins included the PSII core D1 and CP43, the antenna Lhcbm5, the PSI core PsaA and PsaC, the cytochrome b_6f subunits PetA and PetB, and the beta-subunit ATPb of the chloroplast ATP synthase. Results are shown in Fig. 4a and b and Fig. S4, which include immunoblots for 2 independent replicates (one shown in Fig. 4a) and their quantification relative to the continuous light control.

D1 and CP43 were very low (D1) or not detected (CP43) in the dark and increased progressively after 3 to 6 h to levels similar to the continuous light control after 24 to 48 h. Lhcbm5 was very low in the first 6 h and increased thereafter to reach levels similar to the control at 48 h. PsaA and PsaC were not detected (PsaA) or very lowly accumulated (PsaC) in the dark and increased progressively after 3 to 6 h to levels similar to the control at 48 h. PetA and PetB were already detected in the dark and increased upon illumination to levels comparable to the control after 24 to 48 h. Finally, ATPb was detected in the dark to levels similar or slightly higher compared to the continuous light control and stayed constant throughout the light treatment (Fig. 4a and b; Fig. S4).

Together, our results show that PSI and PSII proteins rapidly accumulated after the light onset, consistent with rapid PS assembly under illumination, concomitant with pigment accumulation (Figs. 2 and 3). b_6f proteins, already present in the dark, further accumulated in the light, correlating with the development of thylakoid membranes (Figs. 2 and 3). In contrast, ATPb was already present in the dark, suggesting that ATPase activity may be essential to facilitate the fast energy production required to assemble the chloroplast. Importantly, in all cases, levels at 24 to 48 h were similar to the continuous light control (Figs 4a and b; Fig. S4), indicating that light induces rapid chloroplast biogenesis, in agreement with the early and progressive gain of chloroplast functionality detected after light onset (Fig. 3). This light-induced accumulation was impaired in the presence of lincomycin, consistent with the role of lincomycin as a repressor of plastid translation (Fig. 4a and b; Fig. S5). Importantly, accumulation of the nuclear protein Lhcbm5 was also affected (Fig. 4a and b; Fig. S5), suggesting that lincomycin might trigger a chloroplast-to-nucleus retrograde signaling, inhibiting expression of photosynthesis-associated nuclear genes (*PhANGs*), and thus preventing accumulation of their encoded proteins. We confirmed this by analyzing expression of the

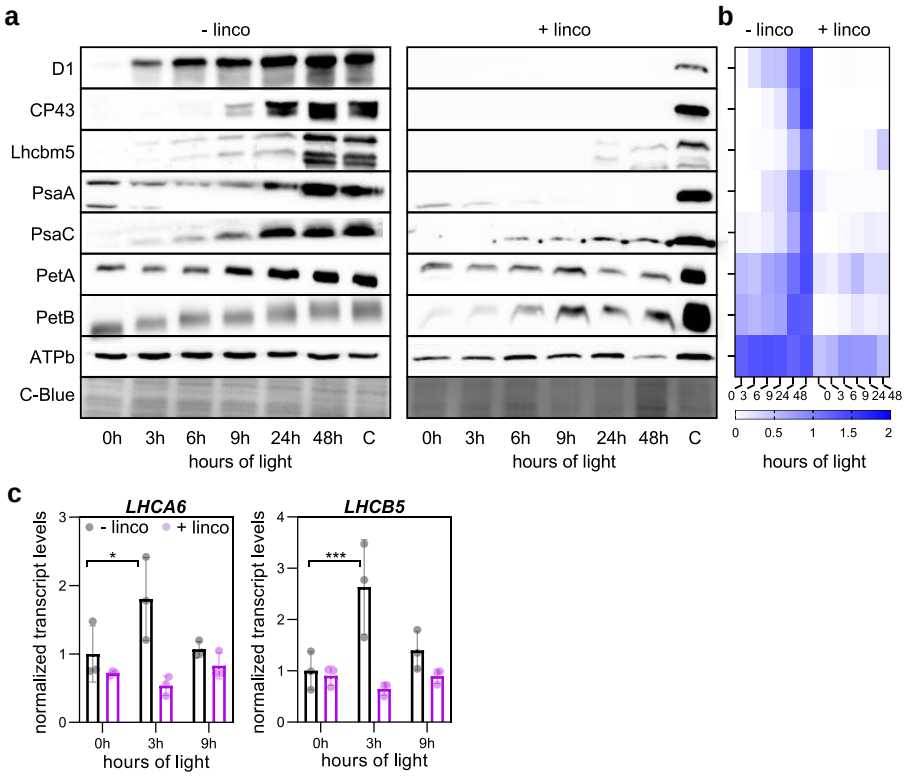

Figure 4 Accumulation of photosynthesis-related proteins during chloroplast biogenesis in *chIL* in the presence or absence of lincomycin. a) Immunoblot analysis of the accumulation of PSII (D1, CP43, and Lhcbm5), PSI (PsaA and PsaC), Cyt b_6f complex (PetA and PetB), and ATP synthase ATPb proteins, in dark-grown *chIL* cells at 0, 3, 6, 9, 24, and 48 h after illumination in the presence (right) or absence (left) of lincomycin (linco). A control (c) corresponding to *chIL* cells grown under continuous light without lincomycin is included. Coomassie blue (C-blue) staining served as a loading control. b) Heatmap of quantified immunoblot data in (a) and 1 additional replicate (Figs. S4 and S5), normalized to each control. c) Transcript levels of *LHCA6* and *LHCB5* analyzed using RT-qPCR in dark-grown *chIL* transferred to light for 0, 3, and 9 h. Data are the means ± SD of biological triplicates ($n = 3$), and asterisks indicate statistically significant differences between the 3 h time point and 0 h (*t*-test; $^*P \leq 0.05$; $^{***}P \leq 0.001$).

Downloaded from academic.oup.com/plphys/article/201/4/kiag600/8762110 by guest on 28 August 2026

PhANGs LHCA6 and *LHCB5* in dark-grown *chlL* cells exposed to light. Indeed, light induced rapid expression of both genes in accordance with their role in chloroplast biogenesis, and this induction was inhibited in the presence of lincomycin (Fig. 4c).

Discussion

Understanding chloroplast biogenesis has long been a key research focus given the importance of photosynthesis and chloroplast metabolism. In angiosperms, chloroplast biogenesis has been widely studied during proplastid-to-chloroplast development (in meristematic cells, monocot leaves, and cell cultures), or etioplast-to-chloroplast development (during seedling de-etiolation, particularly in Arabidopsis) (Jarvis and López-Juez 2013; Hernández-Verdeja et al. 2020; Pipitone et al. 2021). Distinct phases of chloroplast development have been described (Pipitone et al. 2021), in a process controlled by the master regulators GLKs (Hernández-Verdeja and Lundgren 2024). However, the recent discovery of additional regulatory players in *Marchantia polymorpha* (Frangedakis et al. 2024) underscores the value of evolutionary studies in other organisms. In Chlamydomonas, chloroplast biogenesis from a de-differentiated chloroplast occurs during zygospore germination, a process that is challenging to study (Cardador et al. 2025). Consequently, the yellow-in-the-dark *chlL* mutant is an attractive alternative. Here, we have shown that light treatment initiates chloroplast biogenesis in dark-adapted *chlL* cells, in a process that triggers rapid accumulation of pigments, photosynthesis-related proteins, and detection of functional chloroplast activity within hours, based on starch reserves. Interestingly, GLK-like sequences are absent in Chlamydomonas (Hernández-Verdeja and Lundgren 2024), suggesting regulation of chloroplast biogenesis by yet unknown regulators.

Given that chloroplast proteins are encoded by both the plastid and nuclear genomes, coordination of the two is necessary for chloroplast biogenesis (Jarvis and López-Juez 2013). In the light, plastid-to-nucleus retrograde signals (RS) in plants operate during chloroplast biogenesis (biogenic RS), with the plastid-localized pentatricopeptide protein GENOMES UNCOUPLED 1 (GUN1) acting as a key mediator (Pesaresi and Kim 2019; León et al. 2025). Treatment with lincomycin, an inhibitor of plastid translation, has been widely used to study biogenic RS (Martín et al. 2016). Here, we have found that lincomycin specifically affects chloroplast development and physiology in Chlamydomonas, blocking pigment accumulation and photosynthesis, and affecting growth under autotrophic and mixotrophic conditions. In dark-grown *chlL* cells transferred to light, we have shown that lincomycin prevents chloroplast biogenesis, inhibiting protein accumulation as well as the induction of *PhANG* gene expression, therefore establishing lincomycin as a valuable tool for investigating RS and chloroplast biogenesis in Chlamydomonas. The absence of GUN1 in the Chlamydomonas genome (Nishiyama et al. 2018) suggests alternative biogenic RS and mediators (Duanmu et al. 2013).

In summary, our results show that the yellow-in-the-dark *chlL* mutant, carrying a mutation in the CHLL subunit of the DPOR (Suzuki and Bauer 1992), is a powerful model to investigate time-resolved, light-induced chloroplast biogenesis and to explore the poorly understood regulatory mechanisms of chloroplast assembly or the nature of the biogenic RS. By providing a detailed protocol and an initial characterization of the growth, chloroplast biochemistry, and physiology of the dark-adapted *chlL* cells upon light exposure (with and without lincomycin), we aim to facilitate broader use of this model to dissect how PSs assemble and chloroplasts acquire functionalization. This knowledge can inform strategies to enhance photosynthesis, improve stress tolerance, and optimize bioproduct production.

Materials and methods

Strains, media, and growth conditions

C. reinhardtii strains CC-124 and CC-3269, and the *yellow-in-the-dark* mutant CC-3840 (*chlL*) (Suzuki and Bauer 1992), were obtained from http://www.chlamycollection.org and maintained on TAP-agar plates with trace elements (Kropat et al. 2011) at 25 °C in white light (30 μmol m^{-2} s^{-1}). Strains were re-streaked onto fresh TAP-agar plates 1 wk before use. Liquid cultures were grown under white light (50 μmol m^{-2} s^{-1}) or in the dark in TAP or TP media (Harris 2009) with shaking (100 rpm) at 25 °C. Lincomycin (Sigma L6004) diluted in water was used at 0.5 mM. To obtain dark-acclimated cells, colonies were inoculated in TAP liquid medium and grown for 5 d in the dark, with 2 rounds of dilutions and medium refreshment. For dark-to-light transitions, the medium was replaced with fresh TAP on Day 4 at 1 to 2 $\times 10^6$ cells mL^{-1}, when the yellow-in the-dark phenotype was clearly apparent (Fig. 2b). Cultures were divided into 2 flasks, and lincomycin was added into one of them (−17 h). The next day, the medium was replaced with fresh TP (at −3 h), lincomycin was added again to the corresponding flask, and both flasks were kept for 3 h in the dark (Fig. 2b). At 0 h, dark samples were collected. All manipulations during prolonged darkness were done in the dark under safe green light. Finally, cultures were transferred to light (50 μmol photons m^{-2} s^{-1}), and samples were collected over 48 h of light exposure (Fig. 2b).

For WT and *chlL*, standard curves were performed to correlate $OD_{750\ nm}$ values with manually counted cell concentrations, obtaining similar rates for the 2 genotypes in all media and dark/light conditions. We then used $OD_{750\ nm}$ values to estimate cell counts, expressed as millions of cells per milliliter, as indicated in the figures.

Chlorophyll fluorescence-based measurements

In vivo chlorophyll fluorescence was measured at room temperature using a pulse-modulated-amplitude fluorimeter (DUAL-PAM-100, Heinz Walz GmbH, Germany). Measurements were performed in TP medium after 10 min of dark adaptation with stirring. Basal (F_o) and maximum (F_m) fluorescence signals estimated the maximum quantum yield of PSII (F_v/F_m). Measurements of F_m were done in red light (25 μmol photons m^{-2} s^{-1}) by adding 20 μM DCMU. The maximum amount of photo-oxidizable P700 (P_m) corresponds to the change in absorbance at 830 nm relative to 875 nm after application of a saturating red-light pulse (5,000 μmol photons m^{-2} s^{-1}, 200 ms) in a far-red light (75 W m^{-2}) background.

Oxygen evolution and consumption measurements

Oxygen evolution was determined using a Clark-type oxygen electrode (Chlorolab 2+ System; Hansatech, Norfolk, UK) at 25 °C in the presence of 5 mM $NaHCO_3$ under constant stirring. Cells were dark adapted for 5 min, exposed to 50 μmol photons m^{-2} s^{-1} for 5 min, and kept in darkness for 5 min. Respiration was measured as oxygen consumption rate in the dark. The rate of photosynthetic oxygen evolution was calculated as the difference between oxygen evolution in the light and oxygen consumption in the dark, right after the light treatment. Values were normalized to cell number.

Downloaded from academic.oup.com/plphys/article/201/4/kiag600/8762110 by guest on 28 August 2026

Pigment extraction and quantification

Total chlorophylls and carotenoids were extracted in methanol and quantified following Porra et al. (1989) and Lichtenthaler (1987), respectively. Values were normalized to cell number. To generate the chlorophyll and carotenoid absorption spectra, samples were extracted in 85% acetone buffered with 50 mM Tris–HCl (pH = 8) (Chazaux et al. 2022). Pchlide and Chlide were extracted and measured as in Pineau et al. (1986).

Light microscopy

Cells were fixed with 2.5% (v/v) glutaraldehyde (G5882; Sigma-Aldrich) in 50 mM Tris–HCl (pH 7.5) for 1 h at 4 °C, washed with 50 mM Tris–HCl (pH 7.5), and observed using a Zeiss AXIO Scope A1 optical microscope equipped with DIC optics. Images were acquired with an Axiocam 105 camera (Zeiss) and processed using Zen v.2.3 software (Zeiss).

Electron microscopy

Cells were fixed with 2.5% (v/v) glutaraldehyde (G5882; Sigma-Aldrich) in 0.1 M sodium cacodylate buffer (pH 7.4) for 2 h at 25 °C and washed with and postfixed with the same buffer containing 1% (w/v) OsO_4 for 1 h at 4 °C. Fixed cells were stained with 2% uranyl acetate for 2 h, dehydrated through a graded acetone series (from 50% to 100%), and infiltrated with and embedded in Spurr resin (M0300; Sigma-Aldrich). Ultrathin sections (70 nm) obtained using an ultramicrotome (Leica; UC7) were poststained with 2% uranyl acetate, followed by lead citrate, and visualized on a JEOL JEM 1400 Flash electron microscope (JEOL, Tokyo, Japan) operating at 100 kV. Micrographs were taken with a Gatan OneView digital camera (Gatan, California, USA).

Starch extraction and quantification

Cells were treated in 80% ethanol, and the pellet was subjected to alkaline hydrolysis with KOH 0.2 M at 95 °C for 30 min and neutralized with 1 M acetic acid. Starch was further hydrolyzed with amyloglucosidase (Sigma-Aldrich, A7095). Levels were determined indirectly using the glucose oxidase/peroxidase method (Sigma-Aldrich, GAGO20) and normalized to cell number.

Protein preparation and immunobloting

Cells were extracted in lysis buffer (50 mM Tris–HCl, pH 7.5, 2% SDS, 10 mM EDTA, and 1× protease inhibitor cocktail Sigma-Aldrich, 11836153001) at 37 °C for 30 min and quantified with the bicinchoninic acid solution (Sigma-Aldrich; B9643). Fifteen micrograms of protein were subjected to 12% SDS-PAGE and blotted into nitrocellulose membranes (Amersham, 10600003). Antibodies from Agrisera (Vännäs, Sweden) and dilutions used were as follows: D1 (CreCp.g802285_4532) (AS05084, 1:10,000), CP43 (CreCp.g802331_4532) (AS111787, 1:3,000), Lhcbm5 (Cre03.g156900_4532) (AS09408, 1:10,000), PsaA (CreCp.g802280_4532 + CreCp.g802281_4532 + CreCp.g802282_4532) (AS06172, 1:5,000), PsaC (CreCp.g802332_4532) (AS10 939, 1:3,000), PetA (CreCp.g802263_4532) (AS06119, 1:15,000), PetB (CreCp.g802270_4532) (AS184169, 1:7,500), ATPb (CreCp.g802323_4532) (AS05085, 1:5,000), HSP70 chloroplastic (Cre06.g250100_4532) (AS06175, 1:3,000), and HSP70 cytosolic (Cre08.g372100_4532) (AS08371, 1:3,000). An anti-rabbit horseradish peroxidase-conjugated antiserum was used for detection. Blots were developed with the Luminata Crescendo detection system (Millipore, WBLUR0100) and visualized using ImageQuant 800 (Amersham). Densitometric quantification was done with ImageJ (NIH, USA). Data was normalized to levels in control sample, and heatmap was constructed using GraphPad Prism 8 (San Diego, USA).

Gene expression

For quantitative reverse transcription PCR (RT-qPCR), 5 mL of cell culture at a concentration of ~1.5×10^6 was centrifuged at 1,000 × *g* for 5 min, immediately frozen in liquid nitrogen, and stored at −80 °C until processing. Total RNA was extracted using the Maxwell RSC Plant RNA Kit (Promega Corporation; Cat.# AS1500). One microgram of total RNA was used for cDNA synthesis with the NZY First-Strand cDNA Synthesis Kit (NZYtech; Cat.# MB12501), and the obtained cDNA was diluted to a final concentration of 1 *n*g/μL. qPCR reactions were performed in LightCycler 480 Instrument II (Roche Diagnostic) using PowerUp SYBR Green Master Mix (Thermo Fisher Scientific, Cat.# A25778), with primers at a final concentration of 300 nM and 3 μL of cDNA template. Gene expression was measured in 3 independent biological replicates, with 2 technical replicates per biological sample. Relative transcript levels were normalized to RACK1/CβLP as an internal reference gene. Primers used were EMP1758 (5′-CCTGTTT CCCGGGTTTTTGC-3′) and EMP1759 (5′-TTCCACTCTGTCCAACCACC-3′) for LHCA6 (Cre06.g278213_4532); EMP2329 (5′-CATGCGCCAGCATA TAGATAGA-3′) and EMP2330 (5′-CACGCGGCAATCAAAGAAC-3′) for LHCB5 (Cre16.g673650_4532); and EMP1270 (5′-CAAGTACACCATTG GCGAGC-3′); and EMP1271 (5′-CTTGCAGTTGGTCAGGTTCC-3′) for RACK1/CβLP (Cre06.g278222_4532).

Statistical analysis

The physiological parameters shown in Fig. 1d were analyzed using an unpaired *t*-test with Welch's correction, assuming a Gaussian distribution and unequal variances. To identify differences at the gene expression level between 2 time points (0 and 3 h light) in Fig. 4c, the same *t*-test was performed following data treatment specifications in Monte et al. (2004). Asterisks denote statistically significant differences.

Acknowledgments

We thank Alizée Malnoë for her suggestion to employ the *yellow-in-the-dark* mutants in our research, Manuel J. Mallén-Ponce for his expert guidance on photosynthetic measurements and constructive scientific discussions, and Pablo Pulido for support with the transmission electron microscopy (TEM) analysis. We thank Cristina Vaquero, Miguel Barragán, and Beatriz Martín at the electron microscopy (EM) services of CITIUS-US and CNB for EM sample preparation and visualization.

Author contributions

M.Á.R.-S., M.A.D.S., and E.M. conceived the project and designed the experiments. M.Á.R.-S., M.A.D.S., M.B.-T., A.M.Q.-M., B.P., and E.M. planned and performed the experiments. M.Á.R.-S., M.A.D.S., and E.M. analyzed the data. M.Á.R.-S., M.A.D.S., J.L.C., and E.M. wrote the manuscript. All authors approved the final version of the manuscript.

Supplementary material

Supplementary material is available at *Plant Physiology* online.

Downloaded from academic.oup.com/plphys/article/201/4/kiag600/8762110 by guest on 28 August 2026

Funding

This work was supported by grants PGC2018–099987-B-I00, PID2021–122288NB-I00, and PID2024-161051NB-I00 to E.M., funded by the Spanish Ministerio de Ciencia, Innovación y Universidades (MICIU)MICIU/AEI/10.13039/501100011033/ and by "ERDF A way of making Europe," and from the CERCA Programme/Generalitat de Catalunya (Project References 2017SGR-718 and 2021SGR-792 to E.M.). We acknowledge financial support from the Spanish Ministry of Economy and Competitiveness, through the "Severo Ochoa Programme for Centres of Excellence in R&D" CEX2019–000902-S funded by MCIN/AEI/10.13039/501100011033. We also acknowledge financial support from the Junta de Andalucía (grant PAIDI 2021-PROYEXCEL_00587) and the University of Sevilla under the Plan Propio de Investigación y Transferencia program (VI-PPIT and VII-PPIT) to M.Á.R-S., and from MICIU (grants PID2021-123500NB-I00 and TED2021-130912B-I00) to J.L.C. M.Á.R.-S. received postdoctoral funding from the programs Juan de la Cierva Incorporación (MICIU; IJC2018–035773) and Beatriu de Pinós (AGAUR & Marie Sklowdowska-Curie Actions; 2018 BP 0032). M.A.S. was supported by the predoctoral program AGAUR-FI ajuts (2020 FI_B_00343) of the Secretariat of Universities and Research of the Department of Research and Universities of the Generalitat of Catalonia and the European Social Plus Fund. B.P. is a recipient of the predoctoral fellowship HORIZON-MSCA-2021-COFUND-01 rePLANT GA101081581, funded by the European Union and co-funded by the grant CEX2019-000902-S, funded by MICIU/AEI/10.13039/501100011033.

Conflicts of interest

All authors declare no competing interests.

Data availability

All data supporting the findings of this study are available within the article and its supplementary materials published online.

References

Armstrong GA. 1998. Greening in the dark: light-independent chlorophyll biosynthesis from anoxygenic photosynthetic bacteria to gymnosperms. *J Photochem Photobiol B*. 43:87–100. https://doi.org/10.1016/S1011-1344(98)00063-3.

Broderson M, Niyogi KK, Iwai M. 2024. Macroscale structural changes of thylakoid architecture during high light acclimation in Chlamydomonas reinhardtii. *Photosynth Res*. 162:427–437. https://doi.org/10.1007/s11120-023-01067-1.

Cahoon AB, Timko MP. 2000. yellow-in-the-dark mutants of Chlamydomonas lack the CHLL subunit of light-independent protochlorophyllide reductase. *Plant Cell*. 12:559–568. https://doi.org/10.1105/tpc.12.4.559.

Cardador M *et al.* 2025. Extensive remodeling during Chlamydomonas reinhardtii zygote maturation leads to highly resistant zygospores. *Plant J*. 121:e17238. https://doi.org/10.1111/tpj.17238.

Chazaux M, Schiphorst C, Lazzari G, Caffarri S. 2022. Precise estimation of chlorophyll a, b and carotenoid content by deconvolution of the absorption spectrum and new simultaneous equations for Chl determination. *Plant J*. 109:1630–1648. https://doi.org/10.1111/tpj.15643.

Duanmu D *et al.* 2013. Retrograde bilin signaling enables Chlamydomonas greening and phototrophic survival. *Proc Natl Acad Sci U S A*. 110:3621–3626. https://doi.org/10.1073/pnas.1222375110.

Dubreuil C *et al.* 2018. Establishment of photosynthesis through chloroplast development is controlled by two distinct regulatory phases. *Plant Physiol*. 176:1199–1214. https://doi.org/10.1104/pp.17.00435.

Floris D, Kühlbrandt W. 2021. Molecular landscape of etioplast inner membranes in higher plants. *Nat Plants*. 7:514–523. https://doi.org/10.1038/s41477-021-00896-z.

Frangedakis E *et al.* 2024. MYB-related transcription factors control chloroplast biogenesis. *Cell*. 187:4859–4876.e22. https://doi.org/10.1016/j.cell.2024.06.039.

Gillott MA, Erdös G, Buetow DE. 1991. Light-induced chloroplast differentiation in soybean cells in suspension culture: ultrastructural changes during the bleaching and greening cycles. *Plant Physiol*. 96:962–970. https://doi.org/10.1104/pp.96.3.962.

Gommers CMM, Monte E. 2018. Seedling establishment: a dimmer switch-regulated process between dark and light signaling. *Plant Physiol*. 176:1061–1074. https://doi.org/10.1104/pp.17.01460.

Harris EH. 2001. Chlamydomonas as a model organism. *Annu Rev Plant Physiol Plant Mol Biol*. 52:363–406. https://doi.org/10.1146/annurev.arplant.52.1.363.

Harris EH. 2009. Chlamydomonas in the laboratory. In: Harris EH, Stern DB, Witman GB, editors. *The Chlamydomonas sourcebook*. Vol. 1. 2nd ed. Academic Press. p. 241–301.

Hernández-verdeja T, Lundgren MR. 2024. GOLDEN2-LIKE transcription factors: a golden ticket to improve crops? *Plants People Planet*. 6:79–93. https://doi.org/10.1002/ppp3.10412.

Hernández-Verdeja T, Vuorijoki L, Strand Å. 2020. Emerging from the darkness: interplay between light and plastid signaling during chloroplast biogenesis. *Physiol Plant*. 169:397–406. https://doi.org/10.1111/ppl.13100.

Hunsperger HM, Randhawa T, Cattolico RA. 2015. Extensive horizontal gene transfer, duplication, and loss of chlorophyll synthesis genes in the algae. *BMC Evol Biol*. 15:16. https://doi.org/10.1186/s12862-015-0286-4.

Jarvis P, López-Juez E. 2013. Biogenesis and homeostasis of chloroplasts and other plastids. *Nat Rev Mol Cell Biol*. 14:787–802. https://doi.org/10.1038/nrm3702.

Kropat J *et al.* 2011. A revised mineral nutrient supplement increases biomass and growth rate in Chlamydomonas reinhardtii. *Plant J*. 66:770–780. https://doi.org/10.1111/j.1365-313X.2011.04537.x.

León P, Sierra J, Mcquinn RP. 2025. Deciphering plastid retrograde signals and their roles in plant development. *Curr Opin Plant Biol*. 88:102813. https://doi.org/10.1016/j.pbi.2025.102813.

Lichtenthaler HK. 1987. [34] Chlorophylls and carotenoids: pigments of photosynthetic biomembranes. *Meth Enzymol: Plant Cell Membr*. 148:350–382. https://doi.org/10.1016/0076-6879(87)48036-1.

Malnoë P, Mayfield SP, Rochaix JD. 1988. Comparative analysis of the biogenesis of photosystem II in the wild-type and Y-1 mutant of Chlamydomonas reinhardtii. *J Cell Biol*. 106:609–616. https://doi.org/10.1083/jcb.106.3.609.

Martín G *et al.* 2016. Phytochrome and retrograde signalling pathways converge to antagonistically regulate a light-induced transcriptional network. *Nat Commun*. 7:11431. https://doi.org/10.1038/ncomms11431.

Monte E *et al.* 2004. The phytochrome-interacting transcription factor, PIF3, acts early, selectively, and positively in light-induced chloroplast development. *Proc Natl Acad Sci U S A*. 101:16091–16098. https://doi.org/10.1073/pnas.0407107101.

Nishiyama T *et al.* 2018. The Chara genome: secondary complexity and implications for plant terrestrialization. *Cell*. 174:448–464.e24. https://doi.org/10.1016/j.cell.2018.06.033.

Ohad I, Siekevitz P, Palade GE. 1967a. Biogenesis of chloroplast membranes. I. Plastid dedifferentiation in a dark-grown algal mutant

Downloaded from academic.oup.com/plphys/article/201/4/kiag600/8762110 by guest on 28 August 2026

(Chlamydomonas reinhardtii). *J Cell Biol*. 35:521–552. https://doi.org/10.1083/jcb.35.3.521.

Ohad I, Siekevitz P, Palade GE. 1967b. Biogenesis of chloroplast membranes. II. Plastid differentiation during greening of a dark-grown algal mutant (Chlamydomonas reinhardtii). *J Cell Biol*. 35:553–584. https://doi.org/10.1083/jcb.35.3.553.

Ostermeier M, Garibay-Hernández A, Holzer VJC, Schroda M, Nickelsen J. 2024. Structure, biogenesis, and evolution of thylakoid membranes. *Plant Cell*. 36:4014–4035. https://doi.org/10.1093/plcell/koae102.

Pesaresi P, Kim C. 2019. Current understanding of GUN1: a key mediator involved in biogenic retrograde signaling. *Plant Cell Rep*. 38:819–823. https://doi.org/10.1007/s00299-019-02383-4.

Pineau B, Dubertret G, Joyard J, Douce R. 1986. Fluorescence properties of the envelope membranes from spinach chloroplasts. Detection of protochlorophyllide. *J Biol Chem*. 261:9210–9215. https://doi.org/10.1016/S0021-9258(18)67641-0.

Pipitone R *et al.* 2021. A multifaceted analysis reveals two distinct phases of chloroplast biogenesis during de-etiolation in Arabidopsis. *Elife*. 10:e62709. https://doi.org/10.7554/eLife.62709.

Porra RJ, Thompson WA, Kriedemann PE. 1989. Determination of accurate extinction coefficients and simultaneous equations for assaying chlorophylls a and b extracted with four different solvents: verification of the concentration of chlorophyll standards by atomic absorption spectroscopy. *Biochim Biophys Acta (BBA) – Bioenerg*. 975:384–394. https://doi.org/10.1016/S0005-2728(89)80347-0.

Rolland N, Bouchnak I, Moyet L, Salvi D, Kuntz M. 2018. The main functions of plastids. *Methods Mol Biol*. 1829:73–85. https://doi.org/10.1007/978-1-4939-8654-5_5.

Sager R, Palade GE. 1954. Chloroplast structure in green and yellow strains of Chlamydomonas. *Exp Cell Res*. 7:584–588. https://doi.org/10.1016/S0014-4827(54)80107-8.

Solymosi K, Schoefs B. 2010. Etioplast and etio-chloroplast formation under natural conditions: the dark side of chlorophyll biosynthesis in angiosperms. *Photosynth Res*. 105:143–166. https://doi.org/10.1007/s11120-010-9568-2.

Suzuki JY, Bauer CE. 1992. Light-independent chlorophyll biosynthesis: involvement of the chloroplast gene chlL (frxC). *Plant Cell*. 4:929–940. https://doi.org/10.2307/3869460.

Vedalankar P, Tripathy BC. 2019. Evolution of light-independent protochlorophyllide oxidoreductase. *Protoplasma*. 256:293–312. https://doi.org/10.1007/s00709-018-1317-y.

Waters MT *et al.* 2009. GLK transcription factors coordinate expression of the photosynthetic apparatus in Arabidopsis. *Plant Cell*. 21:1109–1128. https://doi.org/10.1105/tpc.108.065250.

White RA, Hoober JK. 1994. Biogenesis of thylakoid membranes in Chlamydomonas reinhardtii y1 (a kinetic study of initial greening). *Plant Physiol*. 106:583–590. https://doi.org/10.1104/pp.106.2.583.

Downloaded from academic.oup.com/plphys/article/201/4/kiag600/8762110 by guest on 28 August 2026